Transmission and Reflection Correlations of Second Harmonic Waves in Nonlinear Random Media

Johannes F. de Boer,[1] Ad Lagendijk,[1,2] and Rudolf Sprik[1]
[1]*van der Waals–Zeeman Laboratorium, Universiteit van Amsterdam, Valckenierstraat 65, 1018 XE Amsterdam, The Netherlands*
[2]*FOM-Institute for Atomic and Molecular Physics, Kruislaan 407, 1089 SJ Amsterdam, The Netherlands*

Shechao Feng
Department of Physics, University of California, Los Angeles, California 90024
(Received 8 February 1993; revised manuscript received 5 August 1993)

We present theoretical and experimental results of the leading order angular correlations of second harmonic light generated *inside* random media, for both the transmission and reflection geometries. We find the striking result that correlations in reflection of the second harmonic light scales with the sample thickness L, in sharp contrast to the corresponding short-range correlation function in reflection of the fundamental light in the linear scattering regime, which scales with mean free path l^*.

PACS numbers: 42.25.Bs, 42.30.Ms, 42.65.Ky, 78.20.Dj

Multiple scattering of classical waves is a growing field of interest. It covers a wide range of applications, from light to sound waves and electron wave functions in disordered mesoscopic systems. The observation of the enhanced backscattering of light from disordered media [1] and universal conductance fluctuations in mesoscopic conductors [2] has shown the importance of interference effects in the multiple scattering regime, and has served as new impetus for the investigation of Anderson localization of light. Closely connected with the localization of light are the correlation properties in transmission and reflection of light in the diffusive, or multiple scattering regime [3–6]. Many of the interesting linear multiple scattering effects have their nonlinear equivalent. For instance, Agranovich and Kravtsov calculated the enhanced backscattering peak for second harmonic light, and found its magnitude to be much smaller than in the linear optics case [7, 8].

In this Letter we present both theoretical and experimental results for the leading angular correlations ($C^{(1)}$) of the second harmonic light generated inside random media, for both the transmission and reflection geometries. In contrast to the enhanced backscattering peak which is much reduced for second harmonic light, the $C^{(1)}$ correlation function remains a quantity of order unity. We find generally good agreement between theory and experiment. As we shall see, the correlation properties in the nonlinear optics regime exhibit richer and more complex features, as they result from the multiple scattering of both the second harmonic and the fundamental light, as well as the randomness in the second harmonic light generation process inside a powderlike random medium containing nonlinear crystallites. The above mentioned nonlinear effects in multiple scattering are unique to optics and do not have an easily accessible counterpart in electronic wave transport systems. The phase coherent nature in the second harmonic light generation is also distinct from that in the generation and propagation of light in random media with luminescent centers. In the latter case the pump light excites radiating transitions which do not in general have a well defined relative phase relation as long as the stimulated radiation effects can be ignored. As a consequence, speckle patterns do not form, in sharp contrast to the second harmonic generation which we study here.

We will first describe the theoretical results briefly. In a polycrystalline powder sample, the small crystallites are responsible for generation of second harmonic light, as well as for multiple scattering of both the fundamental and generated second harmonic light. For convenience in theoretical treatment, we assume the sample has a waveguide geometry, with a cross-sectional area A corresponding to the area of illumination in the experiment. $N \approx k^2 A$ corresponds to the number of propagating modes (which we label by α), and equals the number of independent speckle spots in the far field that can be observed. The intensity transmission and reflection coefficients $T_{\alpha\beta}$ and $R_{\alpha\beta}$, respectively, give the fraction of the power in the incoming mode α that is coupled to the outgoing mode β. The lowest order correlation function ($C^{(1)}$) in transmission in linear optics, defined as the leading contribution to $C_{\alpha\beta\alpha'\beta'} = \langle \delta T_{\alpha\beta} \delta T_{\alpha'\beta'} \rangle / \langle T_{\alpha\beta} \rangle^2$, with $\delta T_{\alpha\beta} = T_{\alpha\beta} - \langle T_{\alpha\beta} \rangle$, has been calculated some time ago, giving the result (neglecting surface reflection effects) [3]

$$C^{T\,(1)}_{\alpha\beta\alpha'\beta'}(\Delta \mathbf{q}_{\perp\alpha} L) = \left[\frac{\Delta \mathbf{q}_{\perp\alpha} L}{\sinh(\Delta \mathbf{q}_{\perp\alpha} L)} \right]^2 \delta_{\Delta \mathbf{q}_{\perp\alpha}, \Delta \mathbf{q}_{\perp\beta}}. \tag{1}$$

Here the angular brackets denote an ensemble average over the disorder, L is the length of the sample (thickness of slab experimentally), $\mathbf{q}_\perp$ is the transverse wave vector for a given waveguide mode (incoming and outgoing direction experimentally), and the condition $\Delta \mathbf{q}_{\perp\alpha} = \mathbf{q}_{\perp\alpha} - \mathbf{q}_{\perp\alpha'}$ represents the "memory effect."

It can be shown that the $C^{(1)}$ correlation function for

© 1993 The American Physical Society

the one-mode in and one-mode out geometry in reflection is given by the square of the enhanced backscattering intensity function [1, 9], which takes the form

$$C^{R(1)}_{\alpha\beta\alpha'\beta'}(\Delta\mathbf{q}_{\perp\alpha}, l^*, L) = \left[\frac{(L+2z_0)\mathrm{cosech}[\Delta\mathbf{q}(L+2z_0)]}{\Delta\mathbf{q}(l^*L + z_0L - 2z_0l^* + 2z_0^2 - 2l^{*2})} \left\{ \frac{\cosh[\Delta\mathbf{q}(L+2z_0)] - \Delta\mathbf{q}l^* \sinh[\Delta\mathbf{q}(L+2z_0)]}{1-(\Delta\mathbf{q}l^*)^2} \right.\right.$$
$$\left.\left. - \frac{[1+(\Delta\mathbf{q}l^*)^2]\cosh(\Delta\mathbf{q}L) - 2\Delta\mathbf{q}l^*\sinh(\Delta\mathbf{q}L)}{[1-(\Delta\mathbf{q}l^*)^2]^2} \right\} \right]^2 \delta_{\Delta\mathbf{q}_{\perp\alpha},\Delta\mathbf{q}_{\perp\beta}}. \quad (2)$$

This expression is taken from Ref. [10]. Corrections due to internal reflection are accounted for by z_0, $z_0 = l^*(2+6C_2)/(3-6C_1)$, as described by Zhu, Pine, and Weitz [11], where C_1 and C_2 are constants determined by the average refractive index of the medium. It is crucial to include the surface effects for the reflection geometry, as the main contribution to the $C^{R(1)}$ correlation function comes from scattering paths which are only a few transport mean free paths l^* long. This is reflected by the scaling variable $\Delta\mathbf{q}_{\perp\alpha}l^*$ for this function. For the transmission geometry, the average path length $s \sim L^2/l^*$, which gives rise to the scaling variable $\Delta\mathbf{q}_{\perp\alpha}L$, so that surface effects are not so important. Thus we may use the simplest boundary condition to calculate the $C^{T(1)}$ correlation function, as we have done in Eq. (1).

We turn now to the calculation of the leading ($C^{(1)}$) correlation function for the second harmonic light. The physical picture for this correlation function is the following [7, 8]: The fundamental light, which is impinging on the surface of the sample at $z = 0$ from a direction characterized by $\mathbf{q}_{\perp\alpha}$, propagates inside the sample while suffering multiple scattering, thus setting up a sample specific specklelike random amplitude (electrical field function) $E_\omega(\mathbf{r})$. Second harmonic light is generated on the randomly placed (and oriented) microcrystallites, described by a source function $S_{2\omega} = \chi_2(\mathbf{r})[E_\omega(\mathbf{r})]^2$, where the tensor field $\chi_2(\mathbf{r})$ describes the random nonlinear susceptibility of the crystalline powder. This randomly generated second harmonic light then propagates throughout the sample, also being multiply scattered by the disordered powder sample. The reflected and transmitted 2ω light in the far field then exhibits a speckle pattern whose correlations we must calculate.

The diagram for calculating the average second harmonic (SH) intensity is given in Fig. 1(a). The corresponding diagram for the $C^{(1)}$ correlation function is given in Fig. 1(b). Upon evaluating these diagrams, we obtain for the correlation functions for both the transmission geometry as well as the reflection geometry, defined as $C^{T,\mathrm{SH}\,(1)}_{\alpha\beta\alpha'\beta'} = \langle \delta T^{\mathrm{SH}}_{\alpha\beta} \delta T^{\mathrm{SH}}_{\alpha'\beta'} \rangle / \langle T^{\mathrm{SH}}_{\alpha\beta} \rangle^2$ and $C^{R,\mathrm{SH}\,(1)}_{\alpha\beta\alpha'\beta'} = \langle \delta R^{\mathrm{SH}}_{\alpha\beta} \delta R^{\mathrm{SH}}_{\alpha'\beta'} \rangle / \langle R^{\mathrm{SH}}_{\alpha\beta} \rangle^2$, the following simple analytical form:

$$C^{T,\mathrm{SH}\,(1)}_{\alpha\beta\alpha'\beta'}(\Delta\mathbf{q}_{\perp\alpha}L) = \left[\frac{3}{\sinh^2(\Delta\mathbf{q}_{\perp\alpha}L)} - \frac{6}{\Delta\mathbf{q}_{\perp\alpha}L\sinh(2\Delta\mathbf{q}_{\perp\alpha}L)} \right]^2 \delta_{2\Delta\mathbf{q}_{\perp\alpha},\Delta\mathbf{q}_{\perp\beta}}, \quad (3)$$

$$C^{R,\mathrm{SH}\,(1)}_{\alpha\beta\alpha'\beta'}(\Delta\mathbf{q}_{\perp\alpha}L) = \left[\frac{\tanh(\Delta\mathbf{q}_{\perp\alpha}L)}{\Delta\mathbf{q}_{\perp\alpha}L} \right]^2 \delta_{2\Delta\mathbf{q}_{\perp\alpha},\Delta\mathbf{q}_{\perp\beta}}. \quad (4)$$

In calculations leading to the above results an integration over the position of the SH sources $S_{2\omega}$ is performed. In transmission the simplest boundary conditions can be used for the same reason as in the transmission case for the fundamental light. In deriving Eq. (4) we have put $z_0 = 0$, which amounts to the neglect of surface effects. As Berkovits showed recently [12], a nonzero z_0 should be included for finite size samples, leading to the expression

$$C^{R,\mathrm{SH}\,(1)}_{\alpha\beta\alpha'\beta'}(\Delta\mathbf{q}_{\perp\alpha}, l^*, L) = \left[\frac{L^3 \sinh[\Delta\mathbf{q}_{\perp\alpha}(L-2z_0)]\{\sinh^2[\Delta\mathbf{q}_{\perp\alpha}z_0] + \sinh^2[\Delta\mathbf{q}_{\perp\alpha}(L-z_0)]\}}{\Delta\mathbf{q}_{\perp\alpha}\sinh^2[\Delta\mathbf{q}_{\perp\alpha}L]\cosh[\Delta\mathbf{q}_{\perp\alpha}L][(L-z_0)^4 - z_0^4]} \right]^2 \delta_{2\Delta\mathbf{q}_{\perp\alpha},\Delta\mathbf{q}_{\perp\beta}}. \quad (5)$$

As the ratio L/z_0 increases, the surface corrections become less important, and Eq. (5) converges to Eq. (4). In this limit the correlation in reflection is a pure bulk effect. This leads to a striking difference between the SH and the fundamental (linear) correlations in the reflection geometry: The SH correlation in reflection [Eq. (4)] depends, to first approximation, only on the product of the thickness L and the transverse wave vector change $\Delta\mathbf{q}_{\perp\alpha}$; whereas the fundamental correlation in reflection [Eq. (2)] is dominated by $\Delta\mathbf{q}_{\perp\alpha}l^*$. In transmission the half-width of the SH correlation is half the half-width of the fundamental (linear) correlation, while both show an exponential decay with $\Delta\mathbf{q}_\perp L$. Although it is hard to predict the absolute yield of SH light in a random sample, one can easily predict the ratio of the SH intensity in transmission over the SH intensity in reflection because the unknown prefactor is divided out. The ratio $\langle T^{\mathrm{SH}}_{\alpha\beta}\rangle/\langle R^{\mathrm{SH}}_{\alpha\beta}\rangle$ is approximately 1/3 for large L/z_0, upon evaluating the diagram in Fig. 1(a) for both the transmission and reflection geometries (corresponding to the $\Delta\mathbf{q}_\perp \to 0$ limit in the calculation of the correlation functions). This is an interesting theoretical result which deserves further experimental investigation, but will not be

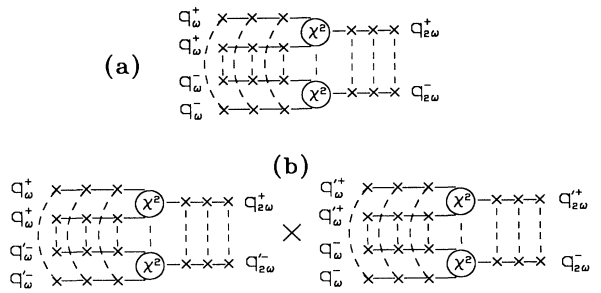

FIG. 1. (a) Feynman diagram for the ensemble average second harmonic intensity transmission and reflection coefficients $\langle T^{\rm SH}_{\alpha\beta}\rangle$ and $\langle R^{\rm SH}_{\alpha\beta}\rangle$. (b) Diagram for the leading order ($C^{(1)}$) correlation function for the second harmonic light, $\langle \delta T^{\rm SH}_{\alpha\beta}\delta T^{\rm SH}_{\alpha'\beta'}\rangle$ or $\langle \delta R^{\rm SH}_{\alpha\beta}\delta R^{\rm SH}_{\alpha'\beta'}\rangle$. Dashed lines connect a series of identical scatterers.

addressed in this paper.

The experimental setup is shown schematically in Fig. 2. A Spectra Physics 3800 Nd:YAG laser was used, giving 90 ps pulses at 1064 nm with a repetition rate of 82 MHz and an average power of 11 W. The beam was chopped and focused to 560 μm on the sample, which consisted of 0.1 to 5 μm $LiNbO_3$ particles on a quartz window. Sample thicknesses were 27, 38, and 65 μm. The average SH intensity was about 15 counts/sec, making it necessary to accumulate signal for 5 sec at each point in an angular scan. The intensity at the fundamental frequency was measured simultaneously by a photodiode. The detectors can be rotated independently from the sample, with an accuracy of 18 μrad and 43 μrad respectively for the detectors and the sample. The sample holder was placed on two translation stages, one to position the sample surface exactly over the rotation axis, and the other to translate the sample perpendicular to the incoming beam to probe different areas of the sample when making multiple scans of the same sample. To ensure detection of only one outgoing mode, polarizers were placed in front of the detectors, and the solid angles seen by the photodetectors for the fundamental and

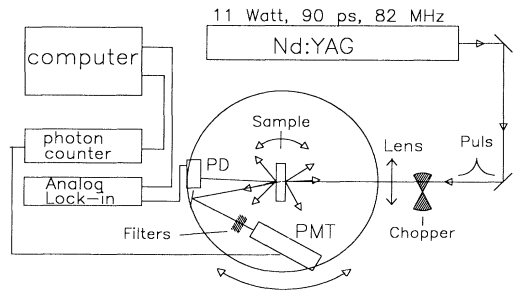

FIG. 2. Experimental setup for recording the angular speckle fluctuations in transmission and reflection. The sample and the detectors can rotate independently over 360 degrees. PMT: photomultiplier (for detecting SH speckles); PD: photodiode (for detecting fundamental light speckles).

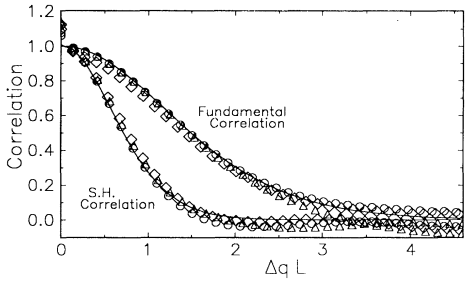

FIG. 3. Fundamental and second harmonic correlation in transmission as a function of sample rotation. Symbols are experimental data for △, $L = 27$ μm; ○, $L = 38$ μm; ◇, $L = 65$ μm, with L the thickness of the sample. Smooth lines: theoretical curves.

the SH light were chosen to be smaller than the solid angle of a single speckle spot. The fluctuating intensity in transmission was recorded as a function of the angle of rotation of the sample. In the reflection measurements the detectors were also rotated to satisfy $\Delta\mathbf{q}_{\perp\alpha} = \Delta\mathbf{q}_{\perp\beta}$ (linear) or $2\Delta\mathbf{q}_{\perp\alpha} = \Delta\mathbf{q}_{\perp\beta}$ (SH). From these scans the (experimental) short-range ($C^{(1)}$) correlation functions were computed.

The mean free path of each sample was determined by measuring the total (linear) transmission coefficient between 1100 nm and 500 nm wavelength, with a Fourier transform infrared spectrometer, using the formula $\langle T\rangle = 2l^*/(L+2l^*)$ [13]. The mean free paths for the different samples which are used for the computation of the correlation in the reflection geometry are given in Table I.

Both in transmission and reflection we were able to observe a clear speckle pattern in the SH light. Figure 3 shows the measured correlation function in transmission for the SH and the fundamental light, together with their respective theoretical curves [from Eqs. (1) and (3)]. The experimental correlation functions were averaged over six to eight scans. The thickness of each sample was determined by fitting the theory to the experimental curves (the only adjustable parameter). The values found agreed within the experimental accuracy of the microscopic thickness determination. We observe that the agreement between theory and experiment is excellent.

Figure 4 shows the measured correlation function in reflection for the SH and the fundamental light, together with their respective theoretical curves [from Eq. (2) and

TABLE I. Values of the mean free paths for the wavelength of 1064 nm (fundamental) and 532 nm (second harmonic) for each sample used in our measurement.

Sample thickness L (μm)	$l^*(\omega)$ 1064 nm (μm)	$l^*(2\omega)$ 532 nm (μm)
27	1.9	1.1
38	3.7	3.2
65	3.4	2.5

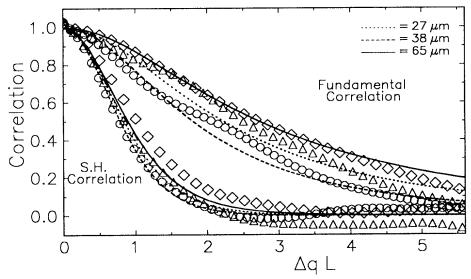

FIG. 4. Fundamental and second harmonic correlation in reflection as a function of sample rotation. The detectors are rotated at twice the angle of the sample rotation. Symbols are experimental data for △, $L = 27$ μm; ○, $L = 38$ μm; ◇, $L = 65$ μm, with L the thickness of the sample. Lines: theoretical curves for the respective sample thicknesses.

Eq. (5)]. The experimental data were averaged over eight to ten scans. The thickness used in the theory is obtained from the transmission experiment. The different theoretical curves for the fundamental correlation reflect their strong dependence on the mean free path. A fit of the average refractive index of the samples to the fundamental reflection data gave $n \approx 1.5$, a relatively high value. This results in $z_0 \approx 2.4l^*$ [11] in Eq. (2) and Eq. (5). The different theoretical curves for the SH correlation are close together, reflecting their scaling behavior with $\Delta\mathbf{q}L$.

In Figs. 3 and 4, the second point of all experimental curves was normalized to 1, rather than the first point, because all the high frequency autocorrelation noise is accumulated in the first point $C(\Delta\mathbf{q}_\perp = 0)$. The experimental data in reflection are in good agreement with the theory. The relative rms fluctuations, defined as the square root of $C(\Delta\mathbf{q}_\perp = 0)$, were between 0.7 and 0.9 for all measurements. The small deviation from the theoretically expected value of unity for this quantity may be attributed to the heating of the sample by the intense fundamental beam, which made the static disorder slightly unstable.

In conclusion, we have studied both theoretically and experimentally for the first time the leading contribution ($C^{(1)}$) to the correlation properties in SH light generated inside a random sample, and shown that the measurements are in good agreement with our theoretical results. The measurements clearly demonstrate the different scale dependence of the SH and fundamental correlation in reflection.

We wish to thank Richard Berkovits and Theo M. Nieuwenhuizen for useful discussions, Ad Wijkstra and Flip de Leeuw for technical support, and Basilio Nesti of Inrad for supplying the $LiNbO_3$ crystals. This work is supported (at Amsterdam) in part by the Stichting voor Fundamenteel Onderzoek der Materie (FOM), which is a part of the Nederlandse Organisatie voor Wetenschappelijk Onderzoek (NWO); and (at UCLA) by the ONR under Grant No. N00014-92-J-4004, the DOE under Grant No. DE-FG03-88ER45378, and the Alfred P. Sloan Foundation.

[1] M.P. van Albada and A. Lagendijk, Phys. Rev. Lett. **55**, 2692 (1985); P.E. Wolf and G. Maret, Phys. Rev. Lett. **55**, 2696 (1985); for recent reviews, see S. John, Comments Condens. Matter Phys. **14**, 193 (1988); *Classical Wave Localization*, edited by P. Sheng (World Scientific, Singapore, 1990); *Analogies in Optics and Micro Electronics*, edited by W. van Haeringen and D. Lenstra (Kluwer, Dordrecht, 1990).

[2] R.A. Webb, S. Washburn, C.P. Umbach, and R.B. Laibowitz, in *Localization, Interaction and Transport Phenomena in Impure Metals*, edited by G. Bergmann, Y. Bruynseraede, and B. Kramer (Springer-Verlag, New York, 1985); in *Mesoscopic Phenomena in Solids*, edited by B.L. Altshuler, P.A. Lee, and R.A. Webb (North-Holland, Amsterdam, 1991).

[3] S. Feng, C. Kane, P.A. Lee, and A.D. Stone, Phys. Rev. Lett. **61**, 834 (1988).

[4] I. Freund, M. Rosenbluh, and S. Feng, Phys. Rev. Lett. **61**, 2328 (1988).

[5] N. Garcia and A.Z. Genack, Phys. Rev. Lett. **63**, 1678 (1989); A.Z. Genack, N. Garcia, and W. Polkosnik, Phys. Rev. Lett **65**, 2129 (1990).

[6] M.P. van Albada, J.F. de Boer, and A. Lagendijk, Phys. Rev. Lett. **64**, 2787 (1990); J.F. de Boer, M.P. van Albada, and A. Lagendijk, Phys. Rev. B **45**, 658 (1992).

[7] V.M. Agranovich and V.E. Kravtsov, Phys. Lett. A **131**, 378 (1988).

[8] V.E. Kravtsov, V.M. Agranovich, and K.I. Grigorishin, Phys. Rev. B **44**, 4931 (1991).

[9] I. Freund, M. Rosenbluh, and R. Berkovits, Phys. Rev. B **39**, 12403 (1989).

[10] The enhanced backscattering intensity function is given by Eq. (68b) in M.B. van der Mark, M.P. van Albada, and Ad Lagendijk, Phys. Rev. B **37**, 3575 (1988). The short-range correlation function for reflection $C^{R(1)}_{\alpha\beta\alpha'\beta'}$ is the square of this (slightly simplified) expression.

[11] J.X. Zhu, D.J. Pine, and D.A. Weitz, Phys. Rev. A **44**, 3948 (1991).

[12] R. Berkovits (private communication).

[13] M.P. van Albada, B.A. van Tiggelen, A. Lagendijk, and A. Tip, Phys. Rev. Lett. **66**, 3132 (1991).